

UNCLASSIFIED

AD 274 269

*Reproduced
by the*

**ARMED SERVICES TECHNICAL INFORMATION AGENCY
ARLINGTON HALL STATION
ARLINGTON 12, VIRGINIA**



UNCLASSIFIED

NOTICE: When government or other drawings, specifications or other data are used for any purpose other than in connection with a definitely related government procurement operation, the U. S. Government thereby incurs no responsibility, nor any obligation whatsoever; and the fact that the Government may have formulated, furnished, or in any way supplied the said drawings, specifications, or other data is not to be regarded by implication or otherwise as in any manner licensing the holder or any other person or corporation, or conveying any rights or permission to manufacture, use or sell any patented invention that may in any way be related thereto.

CATALOGED BY ASTIA
AS AD NO. 274269

ATMOSPHERIC SCIENCE TECHNICAL PAPER NO. 28

ON THE NATURE OF
CLEAR-AIR TURBULENCE (CAT)

by

Elmar R. Reiter

and

Robert W. Hayman

*analysis made
for EOPs
by [unclear]*

Scientific Interim Report
Prepared for Navy Weather Research Facility
Under Contract Number N 189 (188) 538-28A

204 350
Colorado State University Research Foundation
Fort Collins, Colorado



February 1962

CER62ERR11

Atmospheric Science Technical Paper No. 28

ON THE NATURE OF CLEAR-AIR TURBULENCE (CAT)

by

Elmar R. Reiter and Robert W. Hayman

ERRATA

- Page 19, line 7 from bottom: "Up-drafts" instead of "Up-draft"
- Page 22, equation (4): "g" in the denominator instead of " ρ "
- Page 22, line 5 after equation (4): "there" instead of "this"
- Page 22, equation (5): "g" in the denominator instead of " ρ "
- Page 24, equation (6): " ρ_1 " instead of " ρ_i "
- Page 24, line 1 after equation (7): " \bar{u}_1 " instead of " \bar{u}_i "
- Page 24, line 2 from bottom: " ΔT and Δu (m/sec)" instead of " ΔT and m/sec"
- Page 25, line 2 from bottom: "meso-structure" instead of "micro-structure"
- Page 26, line 3 in paragraph 3: "statistics" instead of "statistic"
- Page 27, line 4 from bottom: delete "contribution"

ATMOSPHERIC SCIENCE TECHNICAL PAPER NO. 28

ON THE NATURE OF
CLEAR-AIR TURBULENCE (CAT)

by

Elmar R. Reiter

and

Robert W. Hayman

Scientific Interim Report
Prepared for Navy Weather Research Facility
Under Contract Number N 189 (188) 538-28A

Colorado State University Research Foundation
Fort Collins, Colorado

February 1962

CER62ERR11

Scientific Interim Report, Part I

A PHOTOGRAHMETRIC STUDY OF CLOUD STRUCTURE
ASSOCIATED WITH CLEAR-AIR TURBULENCE

by
Robert W. Hayman

INTRODUCTION

The application of photogrammetric principles to the study of cloud configuration is a unique idea, although not original to this particular project. Examples of this application are to be found in Malkus and Ronne (1), Malkus and Scorer (2), Koschmieder and Neumann (3), Kassander and Sims (4) and Schulz (5). Study of these references revealed that each investigator had used equipment and techniques designed around the particular circumstance of the investigation. For this reason procedures and instrumentation, for this particular study, were selected according to our own requirements and limitations. Discussion of these items comprise Part I of this report.

INSTRUMENTATION

1. Mapping Cameras

The major items of instrumentation, in this particular study, were two K-24 aerial orientation cameras equipped with 178 mm Aero-Ektar lenses. The cameras were selected because of their availability, light weight, optimum focal length, and economy of film requirements. Because the 178 mm lens is, categorically, a narrow angle unit, it was thought that lens distortions would be of negligible amount.

The two cameras were mounted within the framework of a standard engineer's transit. Actually the transit was completely disassembled and the various components modified to suit the requirements. This system enabled

the camera operator to control the attitude of the camera axis in the most general way, and furnished photographic orientation data, regardless of attitude requirement, or the frequency with which this attitude was changed.

2. Whole-Sky Camera System

It was felt that references to a single photograph, taken of a limited segment of a given cloud system, would leave, unanswered, many questions relating to the system, at large. The requirement was thus presented of recording the entire system on a single photograph. This was accomplished by mounting a standard 16 mm movie camera directly over a polished, precision-ground parabolic reflector. The reflector has a circular base, 16 inches in diameter, and was mounted on a rigid platen which could be adjusted to conform to a horizontal plane and oriented to any desired azimuth. The camera lens looked directly into the mirror and was coincident with the axis of the parabola. The view, thus presented to the camera, was one containing the complete horizon and included the total cloud system. The addition of an electronic timer, which actuated a single-framing switch, allowed photographs to be taken at any desired time interval.

3. Coordinate Plotters

Image positions of the various cloud features were precisely measured and recorded through the use of standard, precision comparators, or comparographs. Two such units were made available to this project by Colorado State University. One unit was a David Mann Comparator, capable of direct readings to the nearest 0.001 mm; the other, was a Haag-Streit Comparator, capable of direct reading to the nearest 0.10 mm.

4. IBM 1620 Electronic Computer

The need to investigate many hundreds of object points immediately negated the application of hand calculation methods and arrangements were made to rent computer time for this purpose. The IBM 1620 Computer was available at this institution and was so used. The specific mode of analysis is discussed in subsequent portions of this report.

FIELD CAMERA NETWORK

The locations of the permanent camera sites were chosen to eliminate interference from physical obstruction and the effects of atmospheric contamination found in urban regions. The general site selected was approximately 18 miles northwest of Fort Collins. After considerable study of the area, three specific camera stations were selected. The three stations form the vertices of a triangle with approximate side dimensions of 4.5, 4.1 and 3.2 miles, respectively. The sides of the triangle represent three base lines, whose dimensions provide an important portion of the geometrical analysis of any point in space. The absolute location of two of the points was furnished by the United States Geological Survey, and the third point in the system was located by standard first-order triangulation methods. The descriptions of the three camera locations, in terms of the Colorado State Plane Coordinate System, Northern Zone, were as follows:

Station	Wheat	South	Foundation
X (E-W) Coordinate	2,156,422.4	2,159,408.8	2,175,074.8
Y (N-S) Coordinate	491,471.7	469,831.4	476,785.3
Z (Elev. above MSL)	5,461.1	5,245.9	5,302.5

The positions of space-objects, calculated with respect to any of these three stations, are given with respect to the extension of the aforementioned state plane system, except that effects of the earth's curvature is accounted for in the calculations of elevation of the object.

FIELD METHODS

The K-24 cameras are deployed to two of the three permanent stations. The choice of stations depends, to some extent, on the locations of the cloud systems with respect to the triangle of base lines. The object of the selection is to place the pertinent cloud features on a line extended normal from one of

the three base lines. With the cameras occupying this particular base, and with their axes normal to the base, the objects of interest fall in the central zone of either picture, provided the cloud is a sufficient distance away. As the cloud features are transient, this arrangement cannot be maintained, indefinitely, but nevertheless, represents the optimum of conditions.

The cameras are set up at either end of the chosen base line and each is oriented by backsight to the station occupied by the other. The southernmost of the two cameras is assumed to be oriented at zero azimuth when observing the northernmost station of the particular base line being occupied; the northernmost camera thus reads 180° of azimuth when observing the southernmost unit. Adherence to this scheme means that both units read the same azimuth whenever the axes of the two cameras are parallel in space.

The orientation of the specific features to be photographed is determined by the control camera and this information is relayed to the second unit who then orients on the same feature. Constant communication is maintained, between sites, with standard Citizens Band transceivers.

The analytical reductions which follow the photography do not require that a specific orientation of the two cameras be maintained, relative to one another, or relative to the base line. However, neither camera is allowed, under normal circumstances, to assume a deviation from the normal to the base which is greater than 30 degrees. Rather than sacrificing computational accuracy by exceeding this deviation, one camera would move to the third point of the system, thus utilizing a more favorably oriented base line.

The two cameras are fired manually, but as near to the same instant of time as possible. Each operator observes a precision stop watch which has been synchronized with the other. The time interval of picture taking may vary to suit the rate of change of the features being observed, but is generally standard, for a given series of pictures, at $1/4$ min, $1/2$ min, 1 min or 5 min. Two stop watches are attached to the cameras in such a way that they are included in each picture and fall in some unused zone of the scene. Time differences between the conjugate photos can thus be reduced to inappreciable amounts.

Throughout the entire process, the whole-sky system is providing a continuous recording of the system, at large, into which the individual pictures may be referenced.

DATA REDUCTION

In general, photographic reduction may be accomplished according to one of three basic methods: mathematical, mechanical analogy, or some combination of these. The basic principles involved in any of these techniques have been well tested and, for the most part, are explained in full in standard photogrammetric references. Although the analogies, or semi-analogies are generally more rapid, the mathematical approach was felt to have offered a definite advantage of accuracy for this particular problem, and was so employed.

The basic principle involved is the familiar one of triangulation in space. For any object, recorded on a conjugate pair of photos, the angles of elevation and azimuth are determined by utilizing the known camera locations and orientations and the measured coordinates of the images as recorded on the photographs. The absolute positions and directions of rays emanating from two different locations, toward a common point, are thus established. Solution for the intersection of these rays yields the location, in space, of the desired point. The detailed mathematical model for this analysis is included in the Appendix to Part I of this report.

The sequence of actual reduction is accomplished in the following order:

- a. Identification of points to be analyzed.-- The negative of the left-hand photo is mounted on a light table which is equipped with the Haag-Streit Comparator. The comparator is equipped with a dotting microscope, which enables the operator to pierce the negative along various points of the clouds outline while the scene is being viewed with considerable magnification. Various points in the cloudscape are thus specified by

the system of dots; an arbitrary number is assigned to each dot; the identification is inked directly on the negative.

- b. Transfer of points to the conjugate mate. -- Both negatives of the conjugate pair are oriented beneath a standard mirror stereoscope. The observer causes both views of a single cloud to be superimposed in one scene. The dots from the left-hand photo are then duplicated on the three-dimensional image, thus transferring the specified locations from the left to the right-hand photo. It is felt that an experienced observer will make such a transfer with a probable error not exceeding .02 mm of photographic image position. The effects of this random error is discussed in the general section on errors.
- c. Measurement of image coordinate position. -- The individual negatives are oriented in a standard Mann Comparator. The requirement is that the horizontal and vertical attitudes of the photograph must correspond to the orthogonal directorial motions of the comparator. This is accomplished by reference to a set of horizontal and vertical reference lines that are automatically imposed on the negative at the time of exposure. The reference lines intersect at the principal point of the photo and thus define the origin of coordinate image description. Actual coordinate measurement of the various dots follows very quickly.
- d. Mathematical Analysis. -- The coordinate data is transferred to IBM computer cards; the cards provide a permanent record of the process to this point, and are stored along with the film negatives after processing is complete. In its present form, the Fortran program for image reduction, will handle an indefinite set of data and yields a complete solution of space location in about 4 sec. per object point.

ANALYSIS OF ERRORS

At the outset of this study a simplified theoretical analysis of errors was required in order to evaluate the capacity of the system and also as an aid in selecting some of the variables on which the reduction analysis depends.

In the simplified evaluation of errors, the following assumptions were made:

- a. Both cameras would be oriented with their principal axes normal to the base line;
- b. Both cameras would be placed at the same elevation;
- c. The camera lenses were free from distortion;
- d. The films would not change dimension after exposure.

Reference may be made to any standard photogrammetric text, such as Hallert (6), to obtain the required space-photograph relationships:

$$Y = \frac{Bf}{p} \quad (1)$$

$$X = \frac{Bx'}{p} \quad (2)$$

$$Z = \frac{Bz'}{p} \quad (3)$$

where

X, Y, Z is the coordinate description of the observed object, in space, relative to the left-hand camera;

B is the horizontal distance between the two camera stations;

f is the focal length of the camera lens;

x', z' is the photographic position of object;

p is the parallax of image position, in the x direction.

Parallax is mathematically defined as $(x'_1 - x'_2)$, the difference in x coordinate of the conjugate image.

The error in the Y dimension was chosen for analysis, as it usually represents the largest of the measured quantities. Small errors dB , df and dp are assumed to be present in the base, focal length and parallax measurement. If each term in Eq. (1) is treated separately as we differentiate the expression,

logarithmically, we get

$$dY = \frac{Y dB}{B} = \frac{f dB}{p} \quad (4)$$

$$dY = \frac{Y df}{f} = \frac{B df}{p} \quad (5)$$

$$dY = -\frac{Y dp}{p} = -\frac{Y^2 dp}{Bf} \quad (6)$$

It is apparent that the absolute size of the base influences the accuracy of Y if fixed values are assumed for the other quantities.

Equation (6) may be rearranged in the form

$$\frac{dY}{Y} = \frac{Y dp}{Bf} \quad (7)$$

Without regard to signs, the relative distance error may be examined with respect to base length, parallax error and lens focal length. The focal length was fixed at 178 mm, error in parallax measurement was felt to be in the order of 0.02 mm; a relative distance error of 1/500 was considered acceptable to the nature of the project. Thus

$$\frac{1}{500} = \frac{Y}{B} \cdot \frac{.02}{178}$$

or (8)

$$\frac{Y}{B} \leq 18$$

A base length was then selected which would give a range capacity something greater than 50 miles, with a measurement precision around 1/500. Of course measurements may be made beyond this range, but with a corresponding decrease in precision.

Base lines, corresponding to the given requirements, were then established, as described earlier, and tests were made to evaluate the actual precision capacity of the system. A well defined mountain peak, some 50 miles from the camera stations, was chosen for photographing. The camera orientations were not limited to the specific attitudes assumed in the theory but were allowed to seek random orientations with respect to one another and with respect to the base line. The absolute position of the mountain peak was then computed, according to aforementioned procedures, and the 21 results were statistically compared. A summary of these results is as follows:

Probable error in average X (E-W) dimension - 215 ft.

Ratio of probable error - 1/1085

Probable error in average Y (N-S) dimension - 96 ft.

Ratio of probable error - 1/1410

Probable error in average Z (elevation) dimension - 34 ft.

Ratio of probable error - 1/260

It is emphasized that these statements give an indication of relative accuracy of the system only, since the statistical methods used only compared the photographically measured values with one another. Comparison of photographic description of the point studied with reliable data, furnished by the United States Geological Survey, showed much less favorable error ratios in all cases. The tests revealed a common absolute error of around a mile in X and Y position and errors of around 400 ft in elevation. The author feels that this absolute discrepancy was due, in large part, to the inability to be able to define, photographically, the exact point of given absolute position. It is possible, of course, that some of the fixed error of the test was due to fixed error in the measurement system itself. Continuing investigation will certainly reveal the causes of the fixed errors, and disclose the corrective procedures. Meanwhile, the relative accuracy of points located according to these procedures seems to well exceed the expectations of the investigators.

At the present time, the existing methods of analysis are being refined to further reduce error effects caused by:

- a. Differential film shrinkage;
- b. Localized lens distortions;
- c. Description of camera orientation.

CONCLUSIONS

1. The application of tested photogrammetric principles to the study of cloud configurations appears to be a most practical method of defining a transient and complex system.
2. Relative accuracies of the photogrammetric methods, as employed by the investigators, seem to be well within the requirements of dimensional definition.
3. Absolute accuracy of the system probably warrants further refinement.
4. Cost of these evaluation procedures, exclusive of development, are low enough to allow the continued application of the photogrammetric approach to problems of this nature.

ACKNOWLEDGEMENT

Special acknowledgement is due to Mr. James R. Goodman, Colorado State University, under whose supervision the computer program for this investigation was written and operated. Copies of this program are available, on request from Colorado State University, Department of Civil Engineering.

REFERENCES

1. Malkus, J. S., and C. Ronne, 1954: Concerning the structure of some cumulus clouds which penetrated the high tropical troposphere. Tellus VI, 351-366.
2. Malkus and R. S. Scorer, 1955: The erosion of cumulus towers. Journal of Meteorology, 12, 43-57.
3. Koschmieder, H., and H. G. Neumann, 1957: Zum Lebenslauf von Quellwolken. Beitr. zur Physik der Atmos., 29, 186-208.
4. Kassander, A. R., Jr., and L. L. Sims, 1957: Cloud Photogrammetry with ground-located K-17 aerial cameras. Journal of Meteorology, 14, 43-49.
5. Schulz, H., 1959: Zur Auswertung von WolkenmeBbildern mit elektronischen Rechenautomaten. Beitr. zur Physik der Atmos., 32, 79-83.
6. Hallert, B., 1960: Photogrammetry. New York, Toronto, London. McGraw-Hill Book Co., Inc., 78-84.

APPENDIX TO PART I.

MATHEMATICAL MODEL OF IMAGE-POINT REDUCTION

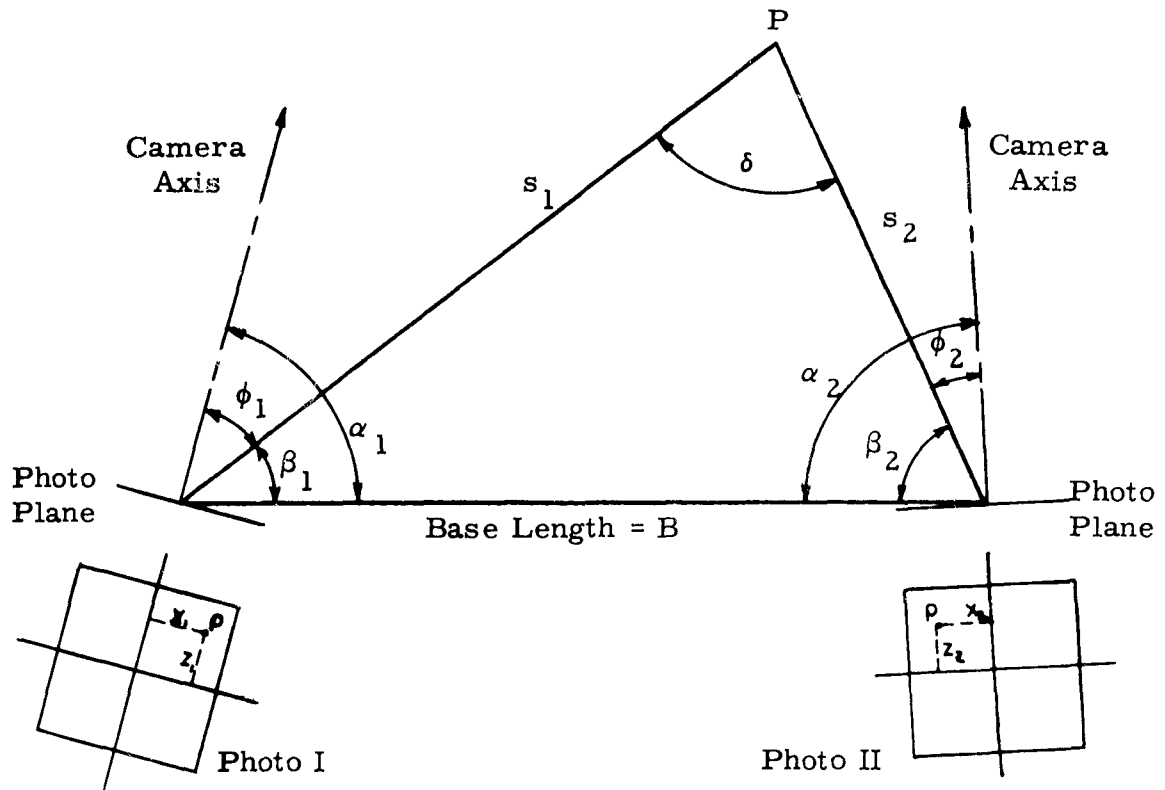


Figure 1.

A point, P , is defined in space if it is visible in two adjacent photographs. If P is in motion, both photographs must be exposed simultaneously.

$\underline{x_1, z_1}$ & $\underline{x_2, z_2}$ are the image coordinates measured from photo I and photo II.

$\begin{cases} x \text{ is plus to the right of the } z \text{ axis} \\ z \text{ is plus above the } x \text{ axis.} \end{cases}$

θ_D is the measured elevation or depression angle of the camera axis.

$\left. \begin{array}{l} \theta_D \text{ is positive as a depression angle.} \\ \theta_D \text{ is negative as an elevation angle.} \end{array} \right\}$

f is the focal length of the camera, stated in millimeters.

ϕ , α , β , δ are defined in Fig. 1.

$$z'_1 = z_1 - f_1 \tan \theta_{D1} \quad \text{and} \quad z'_2 = z_2 - f_2 \tan \theta_{D2} \quad (1)$$

z' = distance from horizon line to p, measured in the plane of
of the photo.

$$z' = z \text{ when } \theta_D = 0$$

$$\phi_1 = \tan^{-1} \left[\frac{x_1}{f_1 \sec \theta_{D1} + z'_1 \sin \theta_{D1}} \right]$$

and $\phi_2 = \tan^{-1} \left[\frac{x_2}{f_2 \sec \theta_{D2} + z'_2 \sin \theta_{D2}} \right] \quad (2)$

ϕ is the horizontal angle between camera axis and point P

(ϕ is plus or minus as x is plus or minus)

$$\beta_1 = \alpha_1 - \phi_1 \quad \text{and} \quad \beta_2 = \alpha_2 - \phi_2 \quad (3)$$

$$s_1 = B \frac{\sin \beta_2}{\sin \delta} \quad \text{and} \quad s_2 = B \frac{\sin \beta_1}{\sin \delta} \quad (4)$$

s = horizontal distance from camera station to P.

(s is given in the units of B, the base length.)

$$\delta = 180 - (\beta_1 + \beta_2)$$

$$v_1 = \frac{z'_1 \cos \theta_{D1} \cos \phi_1}{f_1 \sec \theta_{D1} + z'_1 \sin \theta_{D1}} \quad \text{and} \quad v_2 = \frac{z'_2 \cos \theta_{D2} \cos \phi_2}{f_2 \sec \theta_{D2} + z'_2 \sin \theta_{D2}} \quad (5)$$

v = vertical angle to point P

(v is plus or minus as z' is plus or minus.)

$$X = s \cos \beta \quad (6)$$

$$Y = s \sin \beta \quad (7)$$

$$Z = s \tan v + (2.059 s^2 \times 10^{-8}) \quad (8)$$

X, Y, and Z are given with respect to camera station I or II, according to the subscripts of s, β , and v. The units of X, Y, and Z are the units of the base line. As it stands, X, Y, and Z are the space coordinates of P, referenced to a system whose x axis is coincident with the base line; whose y axis is horizontal, perpendicular to the base line and passing through camera station I or II as desired; and whose z axis is vertical.

X, Y, and Z are converted to the standard state-plane coordinate dimensions \bar{X} , \bar{Y} , \bar{Z} in following manner:

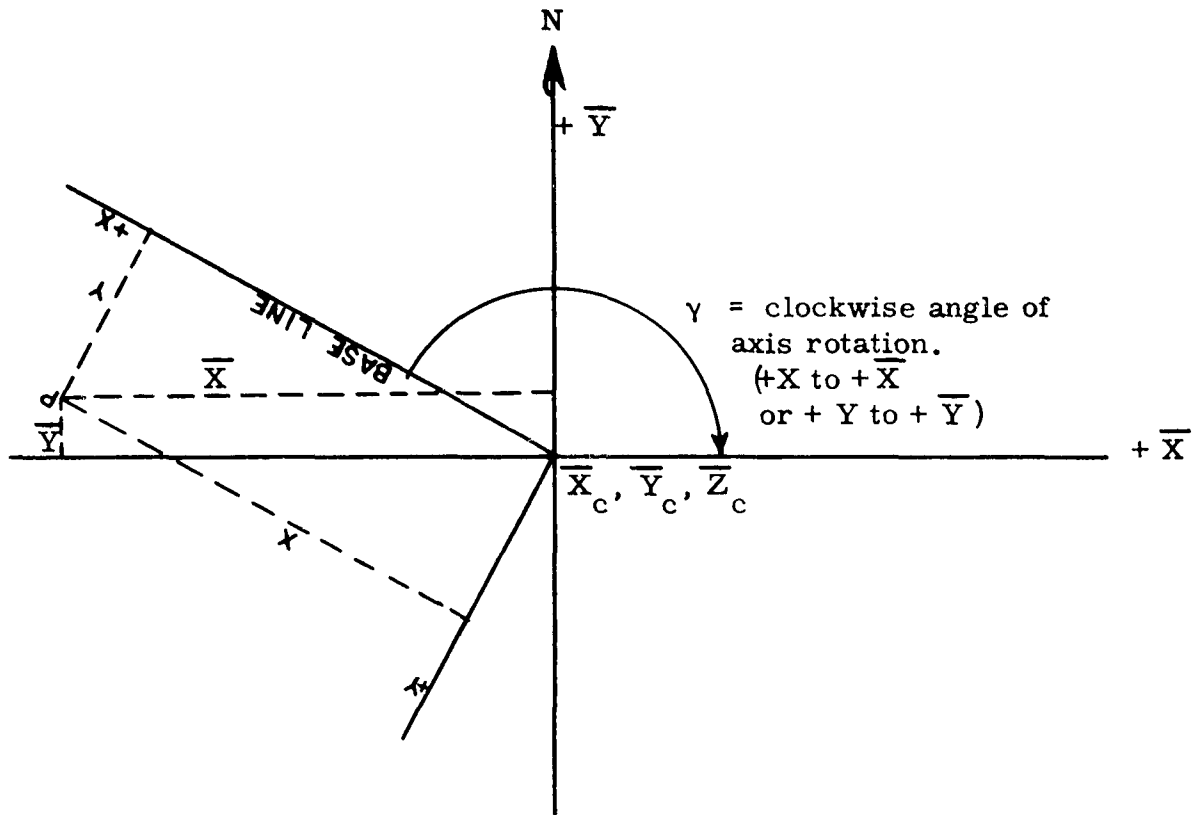


Figure 2.

$$\bar{X} = X \cos \gamma - Y \sin \gamma + X_c \quad (9)$$

$$\bar{Y} = X \sin \gamma + Y \cos \gamma + Y_c \quad (10)$$

$$\bar{Z} = Z + Z_c \quad (11)$$

where \bar{X}_c , \bar{Y}_c and \bar{Z}_c are the standard coordinate descriptions of the control point.

Scientific Interim Report, Part II

ON THE NATURE OF CLEAR-AIR TURBULENCE (CAT)

by

Elmar R. Reiter

INTRODUCTION

Clear-air turbulence still is a phenomenon, which is especially puzzling at times to aviators as well as meteorologists. Not only that it may hit an aircraft rather unexpectedly, but it may also appear with a force, violent enough to constitute one of the major hazards of present-day aviation. It may occur at all levels used by aviation, even in the stratosphere and ozonosphere.

"CAT" is used synonymously to "bumpiness in flight through clear air," which actually would be a better definition of the phenomenon, because of the following two facts:

- a. Many of our CAT data obtained from VGH recordings are difficult to pin-point in space and time. Some of these gusts interpreted as CAT may actually have occurred in thin cirrus or haze layers and thus might not be truly representative for clear-air conditions.
- b. The atmospheric flow, giving rise to CAT, may be completely "laminar" in a hydrodynamic sense. On the other hand, truly "turbulent" flow will not be recorded as CAT, whenever the scale of turbulence elements is below or above certain limiting values.

For convenience sake, we will retain the terminology of "CAT," avoiding a lengthy paraphrase. We shall, however, keep statements 'a' and 'b' in mind when we do so.

If we consider the effect of turbulence on aircraft structure and passenger comfort, statement 'a' becomes irrelevant. For gust-load and stress computations it is of no consequence how the resulting accelerations were brought about.

As shall be pointed out later, bumpiness in flight seems to be most frequently associated with stable and baroclinic layers in the atmosphere. Only with this respect, statement 'a' bears some significance, because the experienced pilot will expect some turbulence in cloud or haze layers, thin as they may be.

A good number of turbulence reports stems from stratospheric levels. As a matter of fact, there does not seem to be any level at all within the atmospheric layer so far used by winged aircraft that were completely void of CAT, not even at operational heights of U-2 and X-15. For tropospheric flow conditions we may visualize part of the CAT to be due to convective and hydrodynamically turbulent motions within adiabatic or even slightly super-adiabatic layers. For the thermodynamically stable stratosphere this source of turbulence will be difficult to realize. There is, however, an increased possibility of CAT wherever the stratosphere shows baroclinicity, according to a modified version of Richardson's criterion (Reiter 1960, Radok et al 1958), which shall be explained further below.

AIRCRAFT IN TURBULENT FLOW

The most readily available reports on high-level turbulence come from aircraft observations. All we can tell with confidence, however, either from pilot reports or from instrument recordings, is that the aircraft experienced a certain amount of accelerations, occurring at certain frequencies. As soon as we try to deduce the magnitude and direction of atmospheric gust velocities responsible for these accelerations, we will have to make certain assumptions on the shape of this gust, which are very difficult to verify (Reiter 1960, and Krumhaar 1958). The most simple version, which, however, is completely suitable to illustrate our problem, assumes a "sharp-edged" gust, i. e., a sharply bounded gust of uniform up- or down-draft, and of infinite extent to one side of the bounding edge. The relationship for the derived vertical gust velocity W_{de} is given by (cf. Pratt 1953)

$$W_{de} = \frac{2b \Delta n}{\rho K a V_i} \quad (1)$$

ρ is the air density, b the wing load (lb/ft^2), Δn the acceleration increment over gravity, in units of gravity, K is a gust alleviation factor (dimensionless), V_i the horizontal true air speed and $a = \frac{dC_A}{d\alpha}$, the change of the lift coefficient C_A with the angle of attack α which depends on the type of aircraft.

As may be seen from expression (1), W_{de} strongly depends on a , and therewith on the specific type of aircraft, which carries out the observations. Generally speaking, the design of slow-flying aircraft offers a larger value of a , than the one of fast-flying jet planes. Thus, with all other conditions assumed equal, the former would experience larger vertical accelerations from the same sharp-edged gusts, than the latter. The fact, however, that the air speed V_i appears in the denominator of expression (1) more than compensates for this effect. Thus, it is usually fast-flying planes, which have more difficulties with CAT.

The fact that fuel burn-off during flight decreases the wing load b continuously, makes the assessment of atmospheric gusts from acceleration records even more difficult.

Furthermore, horizontal and vertical gusts may have similar acceleration effects upon the aircraft, only that the latter usually are four times as powerful than the former, assuming equal gust velocities (Hislop 1951; cf. Reiter 1960a).

The problem becomes even more complex if one considers the elastic properties of the wings, which may by some resonance action exaggerate the effect of atmospheric gusts in certain frequency ranges. This is characterized by the relationship

$$\phi_o(\omega) = [T(\omega)]^2 \phi_i(\omega) \quad (2)$$

$\phi_i(\omega)$ and $\phi_o(\omega)$ are the frequency spectra of input (e.g., atmospheric gust accelerations) and of output (e.g., aircraft accelerations), and $T(\omega)$ is the

frequency-response function which depends on the elastic properties of the aircraft (cf. Krumhaar 1958). Types of airplanes with large and relatively elastic wings, as for instance the U-2, will be particularly sensitive to this kind of exaggerated or distorted "turbulence." If we were concerned with CAT forecasting for one particular type of aircraft only, the foregoing would not concern us much. There is, however, not only a large number of aircraft and missile types to give advice to, but CAT research should also consider future type air vehicles, which may be sensitive to different portions of the perturbation spectrum of the atmosphere. It, therefore, is of paramount importance to: 1) formulate useful working hypotheses on the formation of atmospheric perturbations which may lead to CAT, and 2) collect data on this perturbation spectrum by direct measurements, which do not involve an aircraft. Such measurements can only be carried out by tracking more or less inertia-free bodies, like cloud matter, chaff, or balloons.

A WORKING HYPOTHESIS OF CAT FORMATION

As has been mentioned in the Introduction, CAT may be brought about by hydrodynamically turbulent flow, or by laminar flow as well. Let us define the first as having closed, or almost closed, streamlines in a coordinate system fixed to the earth, and in horizontal and/or vertical planes intersecting the current, indicative of vortex motions within turbulent eddies. The eddies should contain either horizontal or vertical accelerations of a magnitude, which would qualify them as CAT. Among these considerations, convective patterns in the form of Benard cells would qualify. (Up-draft of a magnitude as experienced in Cb - clouds, while satisfying our definition of "turbulence," usually are associated with condensation processes, and do not qualify, therefore, as CAT. The same holds for turbulence observed in orographically produced rotor clouds.) While such situations may occur away from jet streams, where sometimes light turbulence is observed, indeed, it is believed that they would produce only isolated bumps, rather than prolonged "cobblestone" turbulence.

In the vicinity of jet streams, shears usually are too large to permit Benard cells to form. They will be distorted into helical vortices whose stream lines describe a wave pattern in a coordinate system fixed to the earth. This, however, brings us back to "laminar" flow conditions, if we use the definition given above. Assuming perturbations with magnitudes of about 10 percent of the mean flow (= basic current), we realize, that under jet stream conditions they would, at the most, cause fluctuations in the u , v and w components, but never would they lead to a reversal of flow as would have to be the case in real turbulence.

We will, therefore, be quite safe to treat the CAT problem as a wave phenomenon in a current with vertical and/or horizontal gradients of wind speed and/or potential temperature. A good number of theoretical treatments have been forwarded on this subject (cf. Reiter 1960a, 1961a, Clodman et al 1961). It will suffice here to outline only a few basic considerations.

1. Richardson's Criterion

One of the most widely misused criteria in CAT research is the one by Richardson (1920).

$$Ri = \frac{\frac{g}{T} \left(\frac{\partial T}{\partial z} + \Gamma \right)}{\left(\frac{\partial u}{\partial z} \right)^2 + \left(\frac{\partial v}{\partial z} \right)^2} = \frac{\frac{g}{\theta} \frac{\partial \theta}{\partial z}}{\left| \frac{\partial V}{\partial z} \right|^2} \quad (3)$$

g = acceleration of gravity

T = temperature

θ = potential temperature

Γ = dry adiabatic lapse rate

u and v = the components of the wind vector, whose magnitude is V

z = vertical coordinate

Since Richardson derived this expression under laboratory conditions, it will be of rather dubious value for the free atmosphere. It will be even more dubious

when based upon parameters taken from radiosonde ascents, because these, at best, reveal the atmospheric macro-structure, while CAT is a microstructural phenomenon (Reiter 1960a, 1961a).

Nevertheless, we may adopt the position, that Richardson's criterion in essence gives the ratio between the damping forces of vertical thermal stability, and the turbulence generating forces derived from vertical wind shear. Even though the limiting value of $Ri = 1$ derived under laboratory conditions, and separating the turbulent state of flow from the laminar state, will not hold true in the atmosphere, the physical principles underlying the criterion will still be valid. Statistical findings of Petterssen and Swinbank (1947) in the free atmosphere over England suggest a limiting value of 0.65. This ties in nicely with earlier results given by Fage and Falkner (in: Taylor 1932; cf. also Schlichting 1960) who found that the ratio of the exchange coefficient of heat, A_T , to the exchange coefficient of momentum, A_M , for free flow is $\frac{A_T}{A_M} = 2$, while Prandlt's mixing length theory considers these two quantities to be equal, and so does Richardson's criterion. If one computes Ri under the assumption of $\frac{A_T}{A_M} = 1$ (this ratio would appear as a factor on the right-hand side of expression (3)), a limiting value of 0.5 which lies very close to Petterssen's value of 0.65 and which is obtained from considerations of vertical stability and shear only, would be brought back to $Ri = 1$ by applying the factor of $\frac{A_T}{A_M} = 2$ to it.

Expression (3) would indicate increasing probability of turbulence with decreasing vertical stability. This, however, is in disagreement with the frequent observations of CAT at stratospheric levels (Fig. 1, cf. Reiter 1961b). It also contradicts the findings from Project-Jet-Stream analyses, which showed an increase in CAT-frequency within stable and baroclinic layers, such as the "jet-stream fronts" above and below the jet core (Endlich, McLean 1957, Sasaki 1958, Reiter 1960b, 1961c, d, e).

The observations can be made to agree with Richardson's criterion, if the latter is transformed by substituting the vertical wind shear in the denominator of expression (3) by the thermal wind equation (Reiter 1960a, Radok and Clarke 1958). This procedure is irregular insofar as the original Richardson criterion was not meant for motions on a scale that would be influenced by the Coriolis parameter, which appears in the thermal-wind relationship. Nevertheless, this modified criterion has been tested with atmospheric flow conditions, and it seems to show some correlation, at least with the amplitudes of meso-scale perturbations in the jet-stream region (Fig. 2).

With the substitution as outlined, one arrives at

$$Ri^* = \frac{f^2 \theta}{g \frac{\partial \theta}{\partial z} \left[\left(\frac{\partial z}{\partial n} \right)_\theta - \left(\frac{\partial z}{\partial n} \right)_p - \frac{\theta}{\rho} \frac{\partial \dot{V}}{\partial \theta} \right]^2} \quad (4)$$

where the coordinate n is measured normal to the current; the indices θ or p indicate differentiation on an isentropic or isobaric surface, and $\dot{V} = \frac{dV}{dt}$. The last term in the denominator is hard to obtain from observations; it will be dropped, therefore, although it may be of considerable influence on Ri^* , especially in the jet-stream region, where this may be a sizeable vertical gradient of horizontal acceleration. If, furthermore, one neglects the slope of isobaric surfaces against the slope of isentropic surfaces, one obtains the following approximation

$$Ri^* \approx \frac{f^2 \theta}{\rho \frac{\partial \theta}{\partial z} \left(\frac{\partial z}{\partial n} \right)_\theta^2} \quad (5)$$

Expression (5) now states that perturbations are likely to amplify in stable and baroclinic layers. This approximate form of the modified Richardson criterion has been used in constructing Fig. 2.

As may be seen from cross-sections through the jet stream (Reiter 1961b) the baroclinicity in the jet-stream fronts has about the same order of magnitude above and below the jet core, only with reversed sign. Mean vertical wind profiles

in the jet-stream region (Reiter 1958) even seem to indicate, that the wind shear $\frac{\partial V}{\partial z}$ is about 15 to 20 percent stronger on the average above the jet core than below. If we assume isothermal conditions in both, the upper and the lower "jet-stream front" (i. e., the stable and baroclinic layer above and below the jet core), this slightly higher wind shear above the maximum wind level would make the CAT probability according to expression (5) larger in the upper jet-stream front, than in the lower one. There seems to be a slight trend in this direction in the measurements over oceans (Clodman et al), but not so much over continental areas (Sasaki 1958), although the tropopause, and especially the tropopause "break", in any event, harbor a large amount of CAT. Considering that the "tropopause break" actually lies in the region of the upper jet-stream front (Reiter 1960b), this should not be surprising.

The foregoing leaves room for speculation as to possible turbulence at still higher levels of the atmosphere. We know that the polar-night jet at about 25 mb is capable of vertical wind shears of the same magnitude as the polar front or subtropical jet streams (Godson and Lee 1958). This would imply large baroclinicities combined with strong thermal stabilities, as they are characteristic for the stratosphere. While the air density is only about 1/10 of what it is near the tropopause - thus, according to expression (1), reducing the vertical accelerations of the aircraft due to atmospheric gusts to the same fraction - there may still be sufficient energy in small-scale wave perturbations to make it felt as CAT. In this, we will have to consider furthermore, that we still lack knowledge of the spectrum of wave lengths at these heights. Fast-flying aircraft which will operate at these levels will respond to longer wave lengths of perturbations than our present jet aircraft.

2. Waves on Interfaces

The theory of gravity waves on interfaces has already been treated adequately by Helmholtz (1880, 1890). These wave motions may be derived by means of the perturbation method (V. Bjerknes 1926, 1929, 1933; Haurwitz 1941; also Reiter 1961a). One arrives at the following expression for wave

propagation speeds in a shearing current with a temperature discontinuity:

$$C = \frac{\rho_0 \bar{u}_0 + \rho_1 \bar{u}_1}{\rho_0 + \rho_1} \pm \sqrt{\frac{g L}{2 \pi} \cdot \frac{\rho_0 - \rho_1}{\rho_0 + \rho_1} - \frac{\rho_0 \rho_1}{(\rho_0 + \rho_1)^2} (\bar{u}_0 - \bar{u}_1)^2} \quad (8)$$

L being the wave length of the disturbance. Indices 0 stand for the lower layer, 1 for the upper layer. Velocity components \bar{u}_i refer to the basic current. The critical wave-length for which disturbances start to amplify is obtained by equating the expression under the square root to zero. We may also substitute temperature for air density from the equation of state and arrive at

$$L_c = \frac{2\pi}{g} \frac{(u_0 - u_1)^2 \cdot T_0 \cdot T_1}{(T_1 + T_0)(T_1 - T_0)} \quad (7)$$

Abbreviating $\bar{T} = \frac{T_0 + T_1}{2}$, $\Delta T = T_1 - T_0$, $\bar{u}_0 - \bar{u}_1 = \Delta \bar{u}$

we obtain $T_0 \cdot T_1 = \bar{T}^2 - 1/4 (\Delta T)^2$ and

$$L_c = \frac{\pi}{g} \frac{(\Delta \bar{u})}{\bar{T}} \frac{\bar{T}^2 - 1/4 (\Delta T)^2}{\Delta T} \quad (8)$$

Since $1/4 (\Delta T)^2 \ll \bar{T}^2$ we may write

$$L_c = \frac{\pi}{g} \frac{(\Delta \bar{u})^2 \cdot \bar{T}}{\Delta T} \quad (9)$$

For conditions near the tropopause level with $\bar{T} \approx 230^\circ$ we obtain

$$L_c = 73,6 \cdot \frac{(\Delta \bar{u})^2}{\Delta T} \quad (10)$$

The following table (Reiter 1960a) gives values of ΔT and m/sec for different wave lengths.

TABLE 1
Vertical Wind Shear $\Delta \bar{u}$ (m/sec) for Different Temperature
Discontinuities and Critical Wave Lengths at an Interface

ΔT	$L_c = 200$ m	$L_c = 100$ m	$L_c = 50$ m
2°	2.3 m/sec	1.6 m/sec	1.2 m/sec
4°	3.3	2.3	1.6
6°	4.0	2.9	2.0
8°	4.7	3.3	2.3
10°	5.2	3.7	2.6

It should be realized that the atmosphere usually shows a detailed structure, especially near jet streams, consisting of shallow (< 1000 ft thick) stable and baroclinic layers interspersed with less stable layers. The (potential) temperature contrast across these stable layers frequently is of the order of 2 to 4° C. The wind shear necessary to set up waves of a length which would make them felt as CAT is of the same order as meso-scale wind fluctuations so abundantly found during Project-Jet-Stream flights (Reiter, op. cit.).

As Table 1 also shows, the critical wave length is rather sensitive to small changes in shear and in temperature contrast between the two layers. As shall be mentioned in the preliminary results of cloud photogrammetry, waves of these wave lengths, which may be observed at cirrus level under jet-stream conditions, change their appearance and configuration very rapidly. They may show up and disappear again in a matter of a few minutes. Considering the findings on atmospheric meso-structure (Reiter, op. cit.) and the sensitivity of expression (10) to such micro-structure, this should not be surprising at all. It may also help to explain the patchiness of CAT.

More refined treatments of wave formation, using three-layer models with a transition zone instead of a sharp discontinuity have been proposed by Sekera (1948) and Sasaki (1958). While they may serve to elucidate some detailed mechanisms of wave formation and behavior, they will not change materially the basic context of above discussion, which was aimed to point out the significance of gravity and shearing waves for CAT formation.

3. Results of CAT - Statistics

Figure 1 shows no significant preference of light CAT for any particular quadrant around the jet core of the Project-Jet-Stream flights used for this statistic. It became evident, however, that all cases of moderate and severe CAT were located in, or very close to, the axis of a downward drop of the isentropic surfaces - the "isentrope trough."

The explanation for this phenomenon may be sought in the fact, that the "isentrope trough" is produced by sinking motion, which, in turn, tends to further stabilize existing stable layers.

Assuming adiabatic conditions of flow $\left(\frac{d\theta}{dt} = 0\right)$, and no motion in the y-direction ($v = 0$). We may estimate the cause of local stability changes from the advective terms:

$$\frac{\partial}{\partial t} \left(\frac{\partial \theta}{\partial z} \right) = - \frac{\partial u}{\partial z} \frac{\partial \theta}{\partial x} - u \frac{\partial}{\partial x} \left(\frac{\partial \theta}{\partial z} \right) - \frac{\partial w}{\partial z} \left(\frac{\partial \theta}{\partial z} \right) - w \frac{\partial^2 \theta}{\partial z^2} \quad (11)$$

The first term on the right-hand side of this equation contains the influence of differential temperature advection at different heights, the second term the advection of atmospheric layers with different stability. The third term indicates the effect of differential vertical motion on stability, and the fourth term the influence of vertical motion on curved vertical temperature profiles. The combinations from terms 1 and 2 will have to be estimated from future research flights which offer a better three-dimensional data distribution. Figure 3 may serve as an illustration of the effects of term no. 3. Project-Jet-Stream flight no. 27 experienced severe CAT in the area between about 33° N and $32-1/2^\circ$ N

and 35,000 and 37,000 ft (cf. Fig. 1). Derived gust velocities of up to 35 ft/sec were encountered. At 33° N and between 36,000 and 37,500 ft we obtain

$$\frac{\Delta w}{\Delta z} \cdot \frac{\Delta \theta}{\Delta z} = - \frac{2 \text{ m/sec}}{500 \text{ m}} \cdot \frac{3^{\circ} \text{ C}}{500 \text{ m}} = \frac{-6}{2.5 \times 10^5} = -2 \times 10^{-5} {}^{\circ}\text{C/m sec} \quad (12)$$

This would correspond to a change in lapse rate $\frac{\partial \theta}{\partial t} \frac{\partial \theta}{\partial z}$ of about $+7^{\circ}\text{C}/100 \text{ m hour}$, if the conditions prevailing in this cross-section remained unchanged for this period of time, which would hardly be the case.

Term no. 4, again, is difficult to estimate from the available measurements. The foregoing will suffice, however, to demonstrate, that conditions for CAT may change rapidly in the vicinity of jet streams due to changing stabilities, thus influencing Richardson's number (Eq. 5). The same, of course, holds for the term $\left(\frac{\partial z}{\partial u}\right)_{\theta}$ in that expression. The slope of isentropic surfaces normal to the direction of flow will mainly be influenced by velocity gradients $\frac{\partial w}{\partial n}$ and $\frac{\partial v}{\partial z}$.

Again the accuracy of our presently available data does not permit an evaluation of these terms.

MEASUREMENT OF ATMOSPHERIC PERTURBATIONS

It has been mentioned in the foregoing, that gust velocities obtained from aircraft turbulence records do not permit any far-reaching conclusions as to the perturbation state of atmospheric flow. It was decided, therefore, to investigate photogrammetrically the detailed structure of cirrus clouds, with special attention being paid to small-scale wave phenomena, which might have the same dimensions as they are present in CAT.

The considerations upon which these studies were based are the following:

- a. While at lower levels the energy contribution from the latent heat of condensation and/or sublimation makes a large contribution to vertical circulations and to the amplification of perturbation motions, it was felt, that this contribution will be exceedingly small at the cirrus level,

where dry and moist adiabatics are very close to parallel. Thus, any deductions we may make, that are based on thermal stability of the atmosphere - e. g., considerations as they enter into the derivation of Richardson's number - will need only a small, even negligible, percent correction, when extrapolated to dry air conditions.

- b. Since CAT is a very patchy phenomenon even in the vicinity of a jet stream, it has to be expected, that such wave perturbations in cirrus clouds as we are looking for, will not occur too frequently. According to Sasaki (1958), maximum CAT frequency near jet-stream front and tropopause over the eastern U. S. amounts to about 50 percent of the total flying time being turbulent. On the average, we would expect about 15 percent of flying time to be bumpy near jet streams (cf. also Fig. 1). Assuming that the cirrus clouds observed during a particular jet-stream weather situation, occur at one level, we would expect about the same probability of this wave phenomenon to occur.
- c. The observation site near Fort Collins, Colorado, lies only about 40 miles east of the Continental Divide. Orographically induced perturbations may, therefore, trigger wave formations more frequently than should be expected over level terrain.

1. Qualitative Results of Observations

The following qualitative observations were made on this small-scale wave phenomenon:

- a. Waves of wave lengths estimated to less than 1 km, more probably in the range of 10^2 m, could be observed very clearly in sheets or bands of cirrostratus, when the jet stream is close to the area. Figure 4 shows such waves of somewhat larger length on top of an orographically produced Ci-sheet. (No stereo pair of pictures was available of this case, due to failure of one camera.)
- b. These short "CAT - waves" usually appear embedded into larger standing-lee waves.

- c. The waves seem to travel with cloud speed, i. e., very close to the speed of wind.
- d. These waves are of a highly unstable nature, while the cloud banks in which they appear may last for a long time. These short "CAT - waves" may appear in a certain portion of the main cloud in a matter of a few minutes, and dissipate equally as rapidly. They may show up again in another portion of the same cloud.
- e. In most cases, the crests of these small waves seem to be oriented at an angle $> 45^\circ$, or more nearly 90° , from the direction of flow. Different wave trains with slightly differing orientation and wave length have been observed within the same cloud sheet.
- f. On days, when field measurements were in progress on account of observations of such "CAT - waves," pilot reports from the Rocky Mountain area received over teletype indicated observations of moderate to severe CAT.

2. Preliminary Results of Measurements

So far, the photogrammetric results obtained from the first period of the project are more in the nature of a feasibility study. The equipment and program had to undergo extensive testing, as described in Part I of this report. Furthermore, the spurious nature of the phenomenon under investigation did not make all field trips as fruitful as one might have hoped.

Figures 5 and 6 show a view of the cloud pattern of November 23, 1961, at 11:16 a. m. with and without all reference points entered. It should be mentioned that the streaky bands of cirrus in these photographs are not the "CAT - waves" mentioned earlier.*

*A case showing the latter is still in evaluation and not yet ready for presentation.

A photogrammetric evaluation of pairs no. 23 (no. 23 taken 30 sec. earlier than no. 24) and no. 24 (corresponding to above photographs) is presented in Figs. 7 and 8. The vertical scale in these diagrams has been exaggerated by a factor of 10 in order to bring out some of the observed wave structure more clearly. The undulations of the cloud sheet given by points 7 to 14 in the first of these two diagrams does not bear too much significance since it does not show up in Fig. 8. The same holds for points no. 1 through 6 in Fig. 7. These two features of the cloud structure have not been studied in too much detail, which explains some of the inconsistencies.

Let us turn to the cloud streaks which have been evaluated more closely. The following table lists a few corresponding points from the two diagrams. The reason for the scatter in coordinate changes within this time interval of 30 seconds is to be sought in the fact that several of these cloud streaks have been developing upstream, due to their orographic nature. As is evident from Figs. 7 and 8, a wave length in these streaks of about 28,000 ft in the x-direction is present in both evaluations. The vertical amplitude of those waves seems to be 4000 - 6000 ft.

3. Feasibility of Detailed Cloud Studies in a Wave-Length Range Corresponding to CAT

While the foregoing described a situation with wave lengths that were much larger than would be our concern, it will have to be realized that the observed clouds were far down towards the horizon, hence, at a great distance. The photo-pairs presently in evaluation show waves in the "CAT" range, which were much closer to the station. The wave crests had about the same relative distance from each other, as the ones shown in Figs. 5 and 6. Since the latter gave reasonable results in their analysis, it would follow that a measurement of "CAT" wave lengths in cirrus clouds by photogrammetric methods is feasible, if the photographs are taken not too far away from the zenith. It will be difficult, however, to compute the speeds of these waves by tracing "corresponding" points from one pair of photographs to the next, simply because these points do not

TABLE 2
Coordinates of Corresponding Points in Figs. 7 and 8.

Point No. Fig. 7	Fig. 8	Figure 7 Frame 23			Figure 8 Frame 24								
		x	y	z	x	y	z	Δx	Δy	Δz			
23	27	2066552. 4	790048. 94	41470. 954	2074362. 2	776225. 06	39575. 570	+ 7810.	-13823. 9	-1895. 38			
16	21	2055357. 3	840535. 13	49501. 735	2074571. 5	781095. 53	42249. 965	+19214.	-59439. 6	-7251. 77			
25	30	2068737. 7	778429. 33	39022. 251	2067472. 2	787767. 28	40091. 607	- 1265.	+ 9337. 9	+1069. 35			
32	35	2042639. 1	849042. 91	45343. 284	2056629. 3	804743. 67	41185. 098	+13990.	-44299. 3	-4158. 19			
31	49	2053658. 3	819285. 54	41027. 750	2048753. 4	843546. 56	43332. 471	- 4905.	+24261. 0	+2304. 72			

identify the true motion of cloud matter to a sufficient degree of reliability. In the author's opinion, this is a point of minor importance, however, because it will mainly be the wave-length of the wave phenomenon, that influences the vertical accelerations observed in CAT, and not so much their speed, since the latter will be very close to the speed of wind and therefore will be irrelevant in considering the motion of the aircraft relative to the air.

ACKNOWLEDGEMENT

The author wishes to acknowledge the valuable field work done by Messrs. L. Busch, P. Knodel and R. McQuivey in collecting the data, and the supervision of the experimental part of this project by R. W. Hayman. Discussions with Dr. H. Riehl, Colorado State University, and Mr. A. L. Morris, Navy Weather Research Facility, Norfolk, Va., were of particular value in organizing this research project.

REFERENCES

- Bjerknes, V., 1926: Die Atmosphärischen Störungsgleichungen. Beitr. Phys. d. fr. Atm. 13: 1- 14.
- Bjerknes, V., 1929: Über die hydrodynamischen Gleichungen in Lagrangescher und Eulerscher Form und ihre Linearisierung für das Studium kleiner Störungen. Geofis. Publ. 5(11): 1-43.
- Bjerknes, V., J. Bjerknes, H. Solberg and T. Bergeron, 1933: Physikalische Hydrodynamik, 797 pp, Berlin: Springer.
- Clodman, J., G. M. Morgan, Jr., and J. T. Ball, 1961: High level turbulence. Final Report under Contract No. AF 19(604) - 5208, Sept. 1960, and AWS (MATS) Tech. Rep. 158, 1961.
- Godson, W. L., and R. Lee, 1958: High level fields of wind and temperature over the Canadian Arctic. Beitr. Phys. d. Atmos. 31 (1/2): 40-68.
- Haurwitz, B., 1941: Dynamic Meteorology, New York: McGraw-Hill.
- Helmholtz, H. v., 1888, 1889: Über Atmosphärische Bewegungen. I and II. Sitzungsber. Akad. Wiss, Berlin.
- Helmholtz, H. v., 1890: Die Energie der Wogen und des Windes. Sitzungsber. Akad. Wiss, Berlin.
- Hislop, G. S., 1951: Clear-air turbulence over Europe. J. Roy. Aeronaut. Soc. 55: 185-225.
- Krumhaar, H., 1958: Zusammenfassender Bericht über neuere Untersuchungen zur Frage der Böenbelastung von Flugzeugen. Max-Planck-Inst. f. Strömungsforschg., Goettingen; Mitteilung No. 21.
- Petterssen, S., and W. C. Swinbank, 1947: On the application of the Richardson criterion to large-scale turbulence in the free atmosphere. Quart. Journ. Roy. Met. Soc. 73:335-345.
- Pratt, K. G., 1953: A revised formula for the calculation of gust loads. Tech. Note. NACA, No. 2964.
- Radok, U., and R. H. Clarke, 1958: Some features of the subtropical jet stream. Beitr. Phys. d. Atmos. 31(1/2):89-108.

- Reiter, E. R., 1958: The layer of maximum wind. *J. Meteor.* 15(1):27-43.
- Reiter, E. R., 1960a: Turbulenz im wolkenfreien Raum. (Clear-Air Turbulence). *Berichte d. D. Wetterd.* No. 61.
- Reiter, E. R., 1960b: The detailed structure of the atmosphere near jet streams. *Geofisica Pura e Appl.* 46: 193-200.
- Reiter, E. R., 1961a: Meteorologie der Shahlströme (Jet Streams). 473 pp., Wien: Springer.
- Reiter, E. R., 1961b: Die vertikale Struktur des Strahlstromkernes. *Ber. d. Deutsch. Wetterd.*, Nr. 80 (1962).
- Reiter, E. R., 1961c: Die Nordamerikanische Strahlstromwetterlage vom 23. bis 27. Januar 1957 and Hand von Forschungflügen des Project Jet Stream. *Beitr. Phys. d. Atmos.* 33:244-279.
- Reiter, E. R., 1961d: The detailed structure of the wind field near the jet stream. *J. Meteor.* 18(1): 9-30.
- Reiter, E. R., 1961e: Die Feinstruktur der Shahlströme, Colo. State Univ. *Atmosph. Sci. Tech. Paper No. 22.*
- Richardson, L. F., 1920: The supply of energy from and to atmospheric eddies. *Proc. Roy. Soc. London, A.* 97: 354-373.
- Sasaki, Y., 1958: A theory and analysis of clear-air turbulence. *Texas A and M. Dep. of Oceanogr. and Meteorol. Scientif. Report No. 1. Contract AF 19(604)-1565.*
- Schlichting, H., 1960: Boundary layer theory. p 611 ff. New York; McGraw-Hill.
- Sekera, Z., 1948: Helmholtz waves in a linear temperature field with vertical wind shear. *J. Meteor.* 5:93-102.
- Taylor, G. I., 1932: The transport of vorticity and heat through fluids in turbulent motion. *Proc. Roy. Soc. London, A.* 135:685.

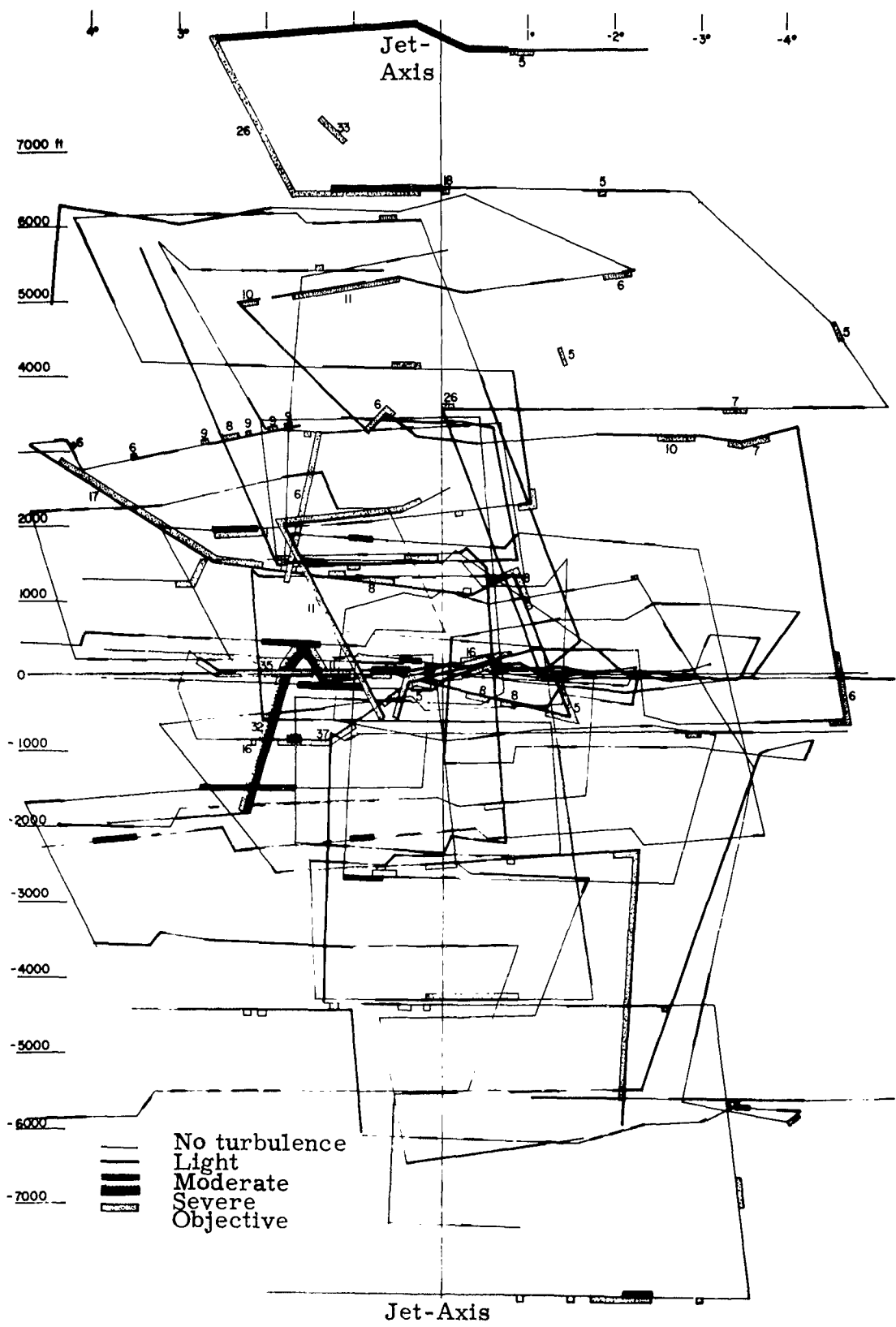


Fig. 1. CAT distribution in 12 Project Jet Stream research flights (Nos. 1, 5, 11, 12, 13, 17, 18, 19, 20, 27, 29 and 30), in a coordinate system based upon the vertical jet axis. Subjective CAT observations: thin lines: no turbulence; medium-weight lines: light turbulence; heavy lines: moderate turbulence; heavy lines with dots: severe turbulence. Objective turbulence measurements: shaded areas; numbers indicate vertical gust velocities in fps.

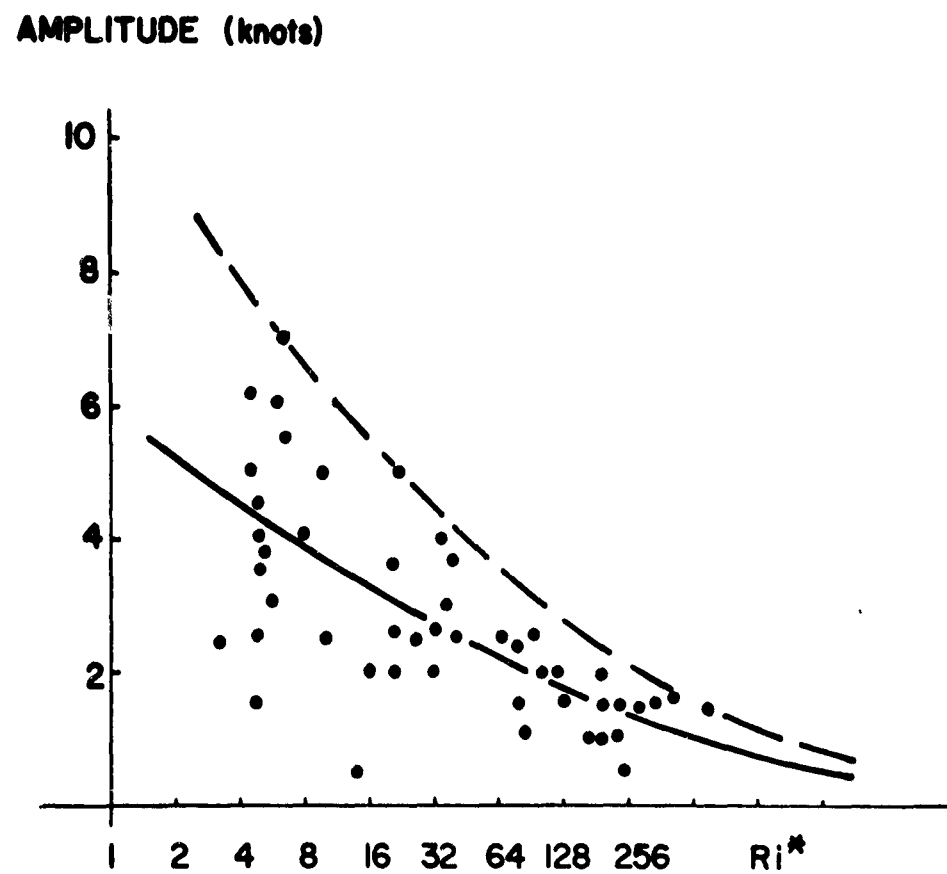


Fig. 2. Correlation of the amplitudes of the mesostructure of wind speed (ordinate) with Ri^* -numbers (abscissa).

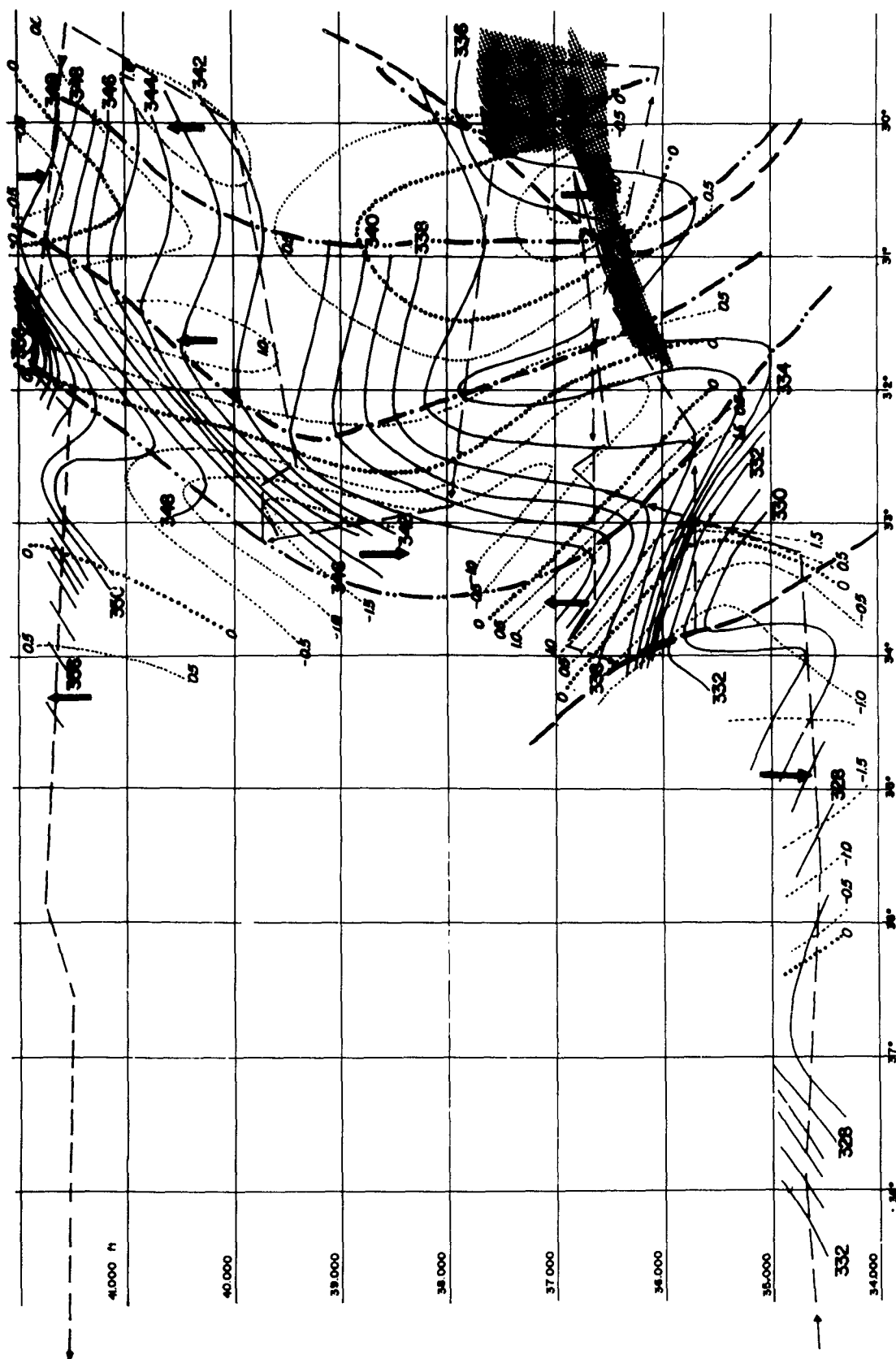


Fig. 3. Isotherms ($^{\circ}\text{K}$) of potential temperature (full lines) and isotachs (m/sec) of vertical motion (dotted) of Project Jet Stream Flight No. 27 March 29, 1957. Flight legs are indicated by thin dashed lines, vertical jet axes by heavy dashed lines, the "isentrope hump" by a dash-dotted line, and the "isentrope trough" by a dash-double-dotted line. Cloud areas are marked by shading.

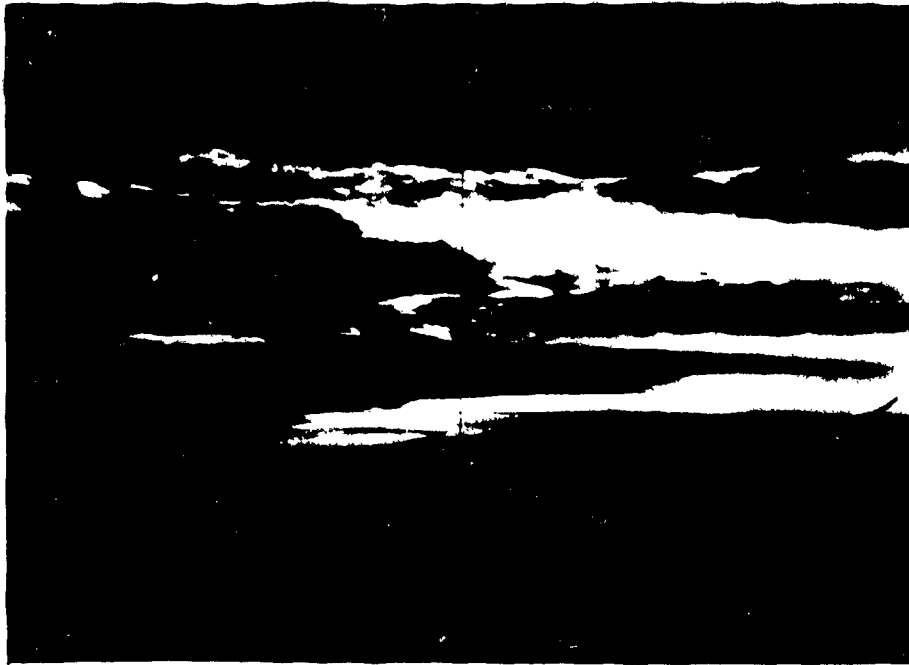


Fig. 4. Clouds seen from camera site "South" on November 3, 1961, ca. 3 p.m. View towards west. Unstable waves on top of an orographically produced sheet of Ci-clouds appear above the center of the photograph. These waves are longer than the usual "CAT-waves", their unstable nature, however, may produce CAT, especially in the wave crests.



Fig. 5. Orographically produced banded Cirrus clouds seen from camera site "South" on November 23, 1961, 11:16 a.m. (Frame Nr. 024.) View towards north.

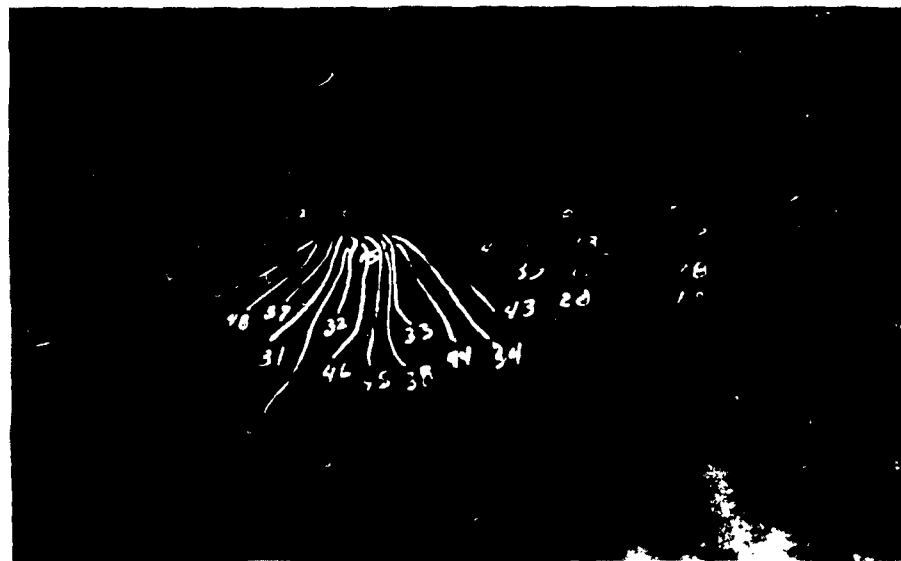


Fig. 6. Same as Fig. 5, except with plotted reference points.

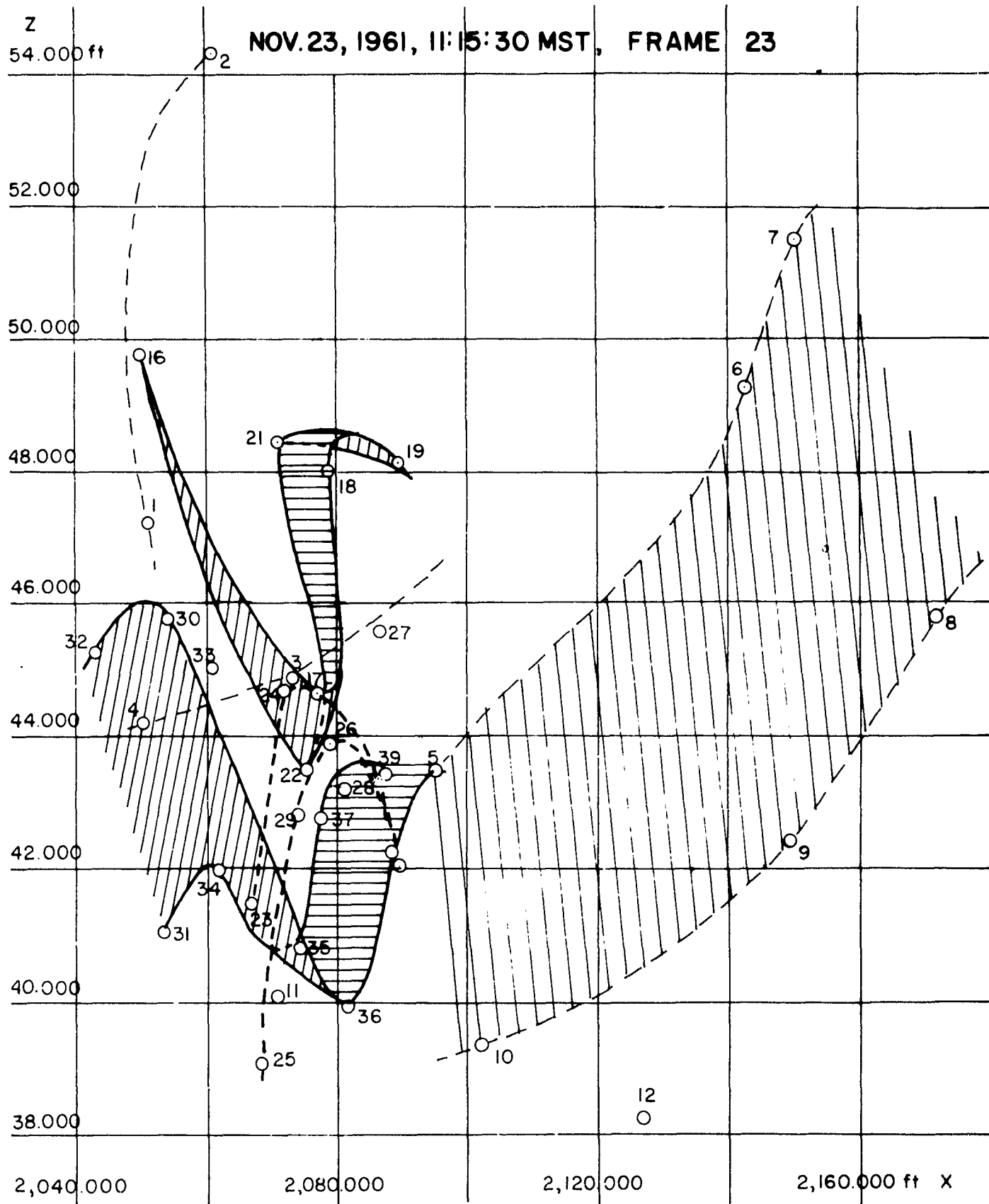


Figure 7. Positions of coordinate points of frame 23 in a vertical plane. The orientation of cloud streaks is indicated by solid and dashed lines and, in part, by shading. The vertical coordinate is exaggerated by a factor of 10.

Z
46.000 ft

NOV. 23, 1961, 11:16 MST. FRAME 24

44.000

49

26 22

32

31

21

28

33

30

27

47

46

29

31

38

36

35

15

45

34

24

37

44

16

7

39

14

42

41

8

12

13

17

19

38.000

36.000

34.000

32.000

2,060,000

16

2,140,000

2,180,000 ft X

Figure 8. Positions of the coordinate points shown in Figure 6 in a vertical plane. The orientation of cloud streaks is indicated by solid and dashed lines, and, in part, by shading. The vertical coordinate is exaggerated by a factor of 10.